POLITECNICO DI TORINO
Repository ISTITUZIONALE

Propagation of toxic substances in the urban atmosphere: A complex network perspective

*Original*
Propagation of toxic substances in the urban atmosphere: A complex network perspective / Fellini, S., Salizzoni, P., Soulhac, L., Ridolfi, L.. - In: ATMOSPHERIC ENVIRONMENT. - ISSN 1352-2310. - ELETTRONICO. - 198:(2019), pp. 291-301. [10.1016/j.atmosenv.2018.10.062]

*Availability:*
This version is available at: 11583/2716997 since: 2018-11-11T12:35:31Z

*Publisher:*
Elsevier

*Published*
DOI:10.1016/j.atmosenv.2018.10.062

*Terms of use:*

This article is made available under terms and conditions as specified in the corresponding bibliographic description in the repository

*Publisher copyright*
Elsevier postprint/Author's Accepted Manuscript

© 2019. This manuscript version is made available under the CC-BY-NC-ND 4.0 license
http://creativecommons.org/licenses/by-nc-nd/4.0/.The final authenticated version is available online at:
http://dx.doi.org/10.1016/j.atmosenv.2018.10.062

(Article begins on next page)

27 November 2026

Elsevier Editorial System(tm) for Atmospheric Environment

Manuscript Draft

Manuscript Number:

Title: Propagation of toxic substances in the urban atmosphere: a complex network perspective

Article Type: Research Paper

Keywords: Urban air pollution; Street network; Complex networks; Vulnerability; Accidental releases; Spreading on networks.

Corresponding Author: Miss Sofia Fellini, M.Eng.

Corresponding Author's Institution: POLITECNICO DI TORINO

First Author: Sofia Fellini, M.Eng.

Order of Authors: Sofia Fellini, M.Eng.; Pietro Salizzoni; Lionel Soulhac; Luca Ridolfi

Abstract: The accidental or malicious release of toxic substances in the urban atmosphere is a major environmental and safety problem, especially in large cities. Computational fluid dynamics codes and simplified modelling tools have been used in the last decades to model pollutant dispersion in urban areas. These studies have shown that propagation is strongly influenced by the layout of buildings and, therefore, by the street topology of the city. This work presents a novel approach to the study of toxic propagation within the urban canopy based on the theory of complex networks. Following recent studies on the development of urban dispersion models, the urban canopy is modelled as a network: the streets and the street intersections represent respectively the links and the nodes of the network. The direction and the weights of the links contain the geometric characteristics of the street canyons and their wind conditions. Within this approach, propagation is modelled as a spreading process on networks and a depth-first search algorithm is used to rapidly delimit the zone of influence of a source node. This zone is the set of streets that are contaminated from the source. As a case study, the proposed model is applied to the urban tissue of the city of Lyon. The algorithm simulates a toxic release in all the nodes of the network and identifies the number of people affected by each propagation process. In this way, vulnerability maps of the city are constructed. Moreover, various wind and concentration scenarios are easily implemented. These results evidence how the proposed method is effective for the rapid assessment of the most vulnerable points in a city, avoiding the use of long numerical simulations.

*Cover Letter

POLITECNICO
DI TORINO

Department of
Environment, Land and
Infrastructure Engineering

Torino, July 16, 2018

To:
Editorial Board of Atmospheric Environment

Subject: Manuscript Submission

Dear Editor,

we are enclosing herewith the manuscript entitled "Propagation of toxic substances in the urban atmosphere: a complex network perspective" for consideration of publication in Atmospheric Environment. With the present submission, we undertake the responsibility that the above-mentioned manuscript is original and has not been published nor is currently under consideration for publication elsewhere.

The research reported in this manuscript proposes an innovative approach for the study of pollutant dispersion within the urban canopy. This new approach is based on the promising theory of complex networks and allows us to model propagation from a source point as a spreading process on networks. In this way, the area of a city affected by a toxic release can be delimited with very low computational costs and vulnerability maps of urban areas can be rapidly constructed.

Our research is of interest for many disciplines, from urban meteorology to complex network science, and makes a significant step forward in the field of atmospheric fluid dynamics. Moreover, our methodology provides interesting tools for relevant current issues like urban pollution mitigation and terrorism prevention. We are thus confident that it is appropriate for publication in Atmospheric Environment.

All authors approved the manuscript and this submission. We know of no conflicts of interest associated with this publication. For any further clarification, do not hesitate to contact us.

We wish to thank you for your consideration and attention.

Best Regards,

Sofia Fellini
Pietro Salizzoni
Lionel Soulhac
Luca Ridolfi

Department of Environment, Land and Infrastructure Engineering
Politecnico di Torino Corso Duca degli Abruzzi, 24 10129 Torino Italia
tel: +39 011.090.5665
sofia.fellini@polito.it www.polito.it

*Manuscript
Click here to download Manuscript: manuscript_Fellini.pdf
Click here to view linked References

# Propagation of toxic substances in the urban atmosphere: a complex network perspective

Sofia Fellini[a,b,*], Pietro Salizzoni[b], Lionel Soulhac[b], Luca Ridolfi[a]

[a] *Department of Environmental, Land, and Infrastructure Engineering, Politecnico di Torino, Corso Duca degli Abruzzi 24, 10129 Turin, Italy*
[b] *Laboratoire de Mécanique des Fluides et d'Acoustique, UMR CNRS 5509, Université de Lyon, Ecole Centrale de Lyon, INSA Lyon, Université Claude Bernard Lyon I, 36, avenue Guy de Collongue, 69134 Ecully, France*

## Abstract

The accidental or malicious release of toxic substances in the urban atmosphere is a major environmental and safety problem, especially in large cities. Computational fluid dynamics codes and simplified modelling tools have been used in the last decades to model pollutant dispersion in urban areas. These studies have shown that propagation is strongly influenced by the layout of buildings and, therefore, by the street topology of the city. This work presents a novel approach to the study of toxic propagation within the urban canopy based on the theory of complex networks. Following recent studies on the development of urban dispersion models, the urban canopy is modelled as a network: the streets and the street intersections represent respectively the links and the nodes of the network. The direction and the weights of the links contain the geometric characteristics of the street canyons and their wind conditions. Within this approach, propagation is modelled as a spreading process on networks and a depth-first search algorithm is used to rapidly delimit the zone of influence of a source node. This zone is the set of streets that are contaminated from the source. As a case study, the proposed model is applied to the urban tissue of the city of Lyon. The algorithm simulates a toxic release in all the nodes of the network and identifies the number of people affected by each propagation process. In this way, vulnerability maps of the city are constructed. Moreover, various wind and concentration scenarios are easily implemented. These results

*Corresponding author
*Email address:* sofia.fellini@polito.it (Sofia Fellini)

evidence how the proposed method is effective for the rapid assessment of the most vulnerable points in a city, avoiding the use of long numerical simulations.

*Keywords:* Urban air pollution, Street network, Complex networks, Vulnerability, Accidental releases, Spreading on networks

## 1. Introduction

Large cities are particularly vulnerable to air pollution as they exhibit both a large number of potential sources and a high density of people exposed (Brunekreef and Holgate, 2002; Heinrich and Wichmann, 2004). Urban air pollution is mainly linked to human activities and in particular to vehicular traffic, heating of buildings and industrial emissions (Mayer, 1999). Moreover, accidental releases such those related to gas leaks, industrial plants or the transport of dangerous goods are particularly critical in densely populated environments. Besides unintentional releases, the current political situation also raises the possibility of terrorist attacks aimed at the dispersal of toxic or pathogenic substances in the air (Tucker, 2000; McLeish, 2017).

For these reasons, local administrations are urged to adopt not only instruments for air quality control but rather predictive tools for the management of dangerous situations due to accidental and malicious releases. These actions are in line with the current challenge of building resilient metropolises able to cope with emergencies (Berke et al., 2009; Ahern, 2011).

Dispersion models are commonly used to predict urban pollution and to estimate concentration of toxic substances. Computational fluid dynamics (CFD) simulations are the most suitable tool for modelling dispersion in a complex geometry like the urban fabric, since they solve the velocity and concentration field in the whole domain (Blocken, 2015). However, these models require a huge computational cost and therefore long simulation times and high performance computers. To reduce the computational cost, several modelling approaches have been developed in the last decades (Di Sabatino et al., 2013). These include street network models (e.g., Carruthers et al., 2000; Soulhac et al., 2011)

based on a simplified description of the building geometry and modelling the mass exchange within and above the urban canopy by parametrising few key transfer processes. Their formulation rely on the basic idea that the urban structure of the city, the orientation of the streets and their connectivity play a major role in determining the intensity of these transfer processes.

Starting from these considerations, this work presents a novel approach for the study of toxic pollutant dispersion within the urban canopy. The aim is to evaluate rapidly and with negligible computational cost the vulnerability of a dense city to the release of harmful airborne pollutants by means of the modern techniques provided by the theory of complex network. According to this perspective, propagation phenomena in the streets are represented as a transport process on a network.

In complex network theory (e.g., Boccaletti et al., 2006; Newman, 2010), complex systems are traced back to a set of entities (nodes) that interact with each other. Interactions are represented as links between the nodes and may have weights that describe the strength of these interactions. Complexity does not lie in the elements that form the system, but rather in their topology and within the pattern of their interconnections. In the last few years, the theory of complex networks has gained a great attention in countless fields, from the social sciences (e.g., Borgatti et al., 2009) to engineering (e.g., Carvalho et al., 2009; Yazdani and Jeffrey, 2011; Giustolisi and Ridolfi, 2014). Recently, a network approach has been adopted for the description of geophysical fluid motion and associated transport phenomena. Gelbrecht et al. (2017) propose a complex network representation of wind flows to study regional meteorology systems, while Ser-Giacomi et al. (2015) represent mixing and dispersion processes in the Mediterranean as a transportation network.

In this work we focus on the pollutant dispersion at the local urban scale. The topology of the city is modelled as a network, within which the propagation of the airborne toxic pollutant occurs. The streets and the street intersections are respectively the links and the nodes of the network. The direction and the weight of the links contain the fluid-dynamics properties of the flow within the

streets and the geometric characteristics of the bordering buildings. In this way, the topology of the city and the wind conditions along the streets are all represented in a single mathematical structure, that is a weighted and directed complex network. Given an initial point, i.e. a pollutant source, the pathways of propagation along the streets can be immediately predicted by this schematic representation. In particular, as in epidemics applications (Newman, 2002), a search algorithm on networks is adopted to delimit the zone of influence of a source node, that we define as the part of the network affected by toxic propagation. By applying this procedure to each node in the network, vulnerability maps can be easily constructed and the urban areas with the highest spreading potential are revealed at a glance. The method is fast and can be applied to entire cities with a low computational cost.

The final aim is to provide a reliable and rapid method to (i) identify the most vulnerable points in the city, i.e. the source points from which the toxic spreading can affect the greatest number of people, and (ii) to understand the effect of wind conditions on urban vulnerability. To this purpose, the methodological tools of network analysis are adopted and long numerical simulation of dispersion processes are avoided.

The work is organized as follows. In Section 2, we describe the physical assumptions adopted to model pollutant propagation in the urban canopy. Then, the network perspective is introduced in Section 3. The basic steps to construct the street network and its weight matrices are thus described and the algorithm for spreading on networks is presented. Subsequently, the proposed general method is applied to the city of Lyon (France). Vulnerability maps for a district of Lyon are shown and analysed in Section 4. Finally, the main conclusions obtained from the presented work are summarized.

## 2. Physical assumptions about the propagation of a toxic substance in the urban environment

Transport and mixing processes in the urban environment are characterized by complex fluid structures due to the interaction between the atmospheric flow and the city. The presence of buildings and vegetation highly affects the structure of the urban boundary layer, characterized by the generation of a shear layer at the top of the canopy, wake diffusion behind buildings, and form drag due to the pressure differences across the roughness elements (Roth, 2000). Moreover, the flow field in the streets is altered by the convective fluxes due to the differential solar irradiance on building walls and to the heat sources related to human activities (Oke, 1982; Arnfield, 2003). The simulation of all these dynamical effects on the flow field within the urban canopy is nowadays a challenge for modellers that adopt sophisticated computational tools, typically CFD codes (Tominaga and Stathopoulos, 2012). These require a huge amount of input data and high computational costs, which limit their use when analysing a large number of emission scenarios. In this latter case, alternative simulation strategies should be adopted, based on a simplified description of the flow and of the dispersion phenomena occurring within the urban fabric.

The physical assumptions for the propagation model presented in this work are based on a street network approach (e.g., Namdeo and Colls, 1996; Soulhac et al., 2011). The geometry of the urban canopy is simplified to a network of streets (Fig. 1.a), and the streets are represented as urban canyons, i.e. cavities of rectangular section with length $l$, height $h$ and width $w$ (Fig. 1.b). Following the approach of Soulhac et al. (2011), the main transport phenomena for a airborne pollutant in the urban canopy are (i) the convective mass transfer along the street due to the mean wind along the longitudinal axis, (ii) the vertical transfer toward the external atmosphere and (iii) the transport at street intersections.

We introduce here two further simplifications to this approach. The first concerns the model for the pollutant transfer at street intersections, which is

significantly different from that adopted by Soulhac et al. (2011). Secondly, we will neglect the dispersion occurring above roof level. Since our focus is on ground level releases only (therefore inducing maximal concentration at the street level, within the canopy), we will assume that the amount of pollutant transferred out of the streets, towards the overlying boundary layer, will not further contribute to the pollutant concentration in the downwind streets. In other words, we consider that this vertical flux of pollutants, from the canopy to to the external atmosphere, will induce negligible concentrations above roof level (due to the high dilution occurring in the lower part of the boundary layer, compared to that within the streets) and that eventual mass flows from the overlying atmosphere towards the street canyons will not contribute significantly to ground level pollution. These two assumptions allow us to adapt the street network approach to the propagation model presented in Section 3 based on the formalism of the theory of complex networks.

In the following, the transport mechanisms along a street canyon and at street intersections are described in details. The emission scenario consists of a ground level and punctual release ($s$ in Fig. 1) within the urban canopy. The external wind blowing on the city with direction $\Phi$ is the driving force for propagation processes.

### *2.1. Transport along a street canyon*

Consider a source $s$ releasing a gaseous substance that results in a concentration $c_0$ at the beginning of a street canyon, as illustrated in Fig. 1.b-c. The substance propagates horizontally due to the advective flux along the longitudinal axis, and vertically due to the turbulent flux between the street and the overlying atmosphere (Soulhac et al., 2013). A simple but exhaustive way to model these two mechanisms is the use of the one-dimensional transport equation

$$\frac{\partial c}{\partial t} + u_{st}\frac{\partial c}{\partial x} + \frac{u_d}{h}(c - c_{ext}) = 0, \tag{1}$$

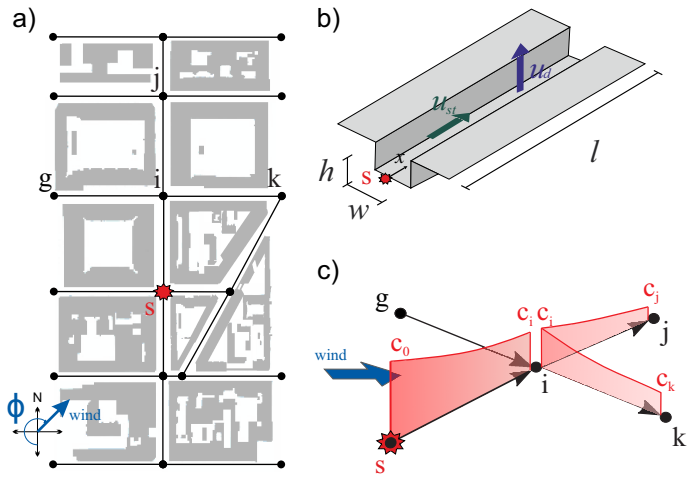


Figure 1: a) Toxic source $s$ within a network of streets. Propagation is driven by the wind blowing on the city with direction $\Phi$. b) Representation of a street canyon with the main variables of the model. c) Transport of a contaminated flow in street intersections.

whose solution is the function $c(x,t)$, i.e. the concentration along the longitudinal coordinate $x$ over time $t$.

The first two terms in (1) describe the convective transport driven by the spatially averaged wind velocity along $x$ ($u_{st}$). This velocity is assumed to be given by a balance between the stress imposed at the canopy top by the external atmospheric flow and the drag due to the roughness of the canyon walls (neglecting the role of pressure gradients). Under this assumption, Soulhac et al. (2008) derived an analytical formulation for $u_{st}$, as a function of the external wind intensity and direction, the geometry of the street canyon and the aerodynamic roughness of building walls (see Appendix A). The third term in (1) models the mass transfer from/to the canyon to/from the overlying atmosphere by means of a bulk exchange velocity $u_d$ (Salizzoni et al., 2009) estimated as

$$u_d = \frac{u_*}{\sqrt{2\pi}}, \tag{2}$$

where $u_*$ is the friction velocity of the overlying boundary layer flow. Assuming that pollutant concentration above the canopy, $c_{ext}$, is negligible compared to the concentration in the canyon, the vertical flux is unidirectional. This vertical

loss is the only decay term in the model, since it is assumed that the involved toxic substances do not undergo chemical or biological transformations or, in any case, have a reaction time longer than the time needed for propagation.

In (1), turbulent longitudinal diffusion is not considered as it is negligible with respect to the longitudinal advection.

Equation (1) was solved for both an instantaneous and a continuous release in the source (see Appendix B). In the first case, the initial condition is set as a rectangular pulse with height $c_0$. The solution describes this initial step travelling along the street with velocity $u_{st}$ and undergoing an exponential decay of concentration. In the second case, the initial condition is a continuous release with constant concentration $c_0$. The solution is a front that spreads along the street with velocity $u_{st}$. Although the analytical solutions are different, the concentration at the end of the street ($x = l$) in both cases is the same:

$$c_l\left(x = l, t = \frac{l}{u_{st}}\right) = c_0 e^{-\frac{l}{u_{st}}\frac{u_d}{h}}. \tag{3}$$

Thus, the concentration at the beginning of the street ($c_0$) undergoes an exponential decay driven by the ratio between the advection time ($l/u_{st}$) that the toxic front spends to reach the end of the street, and the vertical transfer time ($h/u_d$). The terms in the exponent summarize all the information about the geometry of the canyon and the flow dynamics in it.

### *2.2. Transport in the street intersections*

The flow field in the street intersections is driven by complex physical processes that depend on multiple geometric and meteorological parameters. Several studies (e.g. Hunter et al., 1990; Robins et al., 2002; Soulhac et al., 2009) have demonstrated that even slight variations in the building geometry and wind direction can affect significantly the redistribution of the incoming fluxes over the outgoing fluxes. On the basis of these observations, Soulhac et al. (2009) have developed a model, quantifying the balance of the time-averaged incoming and outgoing fluxes at the street intersection, depending on its geometry and

on the direction of the external wind. In defining the exchange model in the intersection for the pollutant propagation within the network we however adopt a different approach. Our aim is twofold: i) adopt a model which is the simplest as possible, and ii) adopt a conservative approach. With these aims we will consider that the concentration of pollutants at the beginning of the streets exiting the intersection is the one at the end of the incoming contaminated canyon.

Consider a simple intersection with a single incoming and one outgoing street canyon. The air flow entering the intersection with a concentration $c_{in}$ is $Q_{in}$, while the air flow outgoing the intersection with a concentration $c_{out}$ is $Q_{out}$. Two cases are possible for the mass balance in the intersection. In the first case, the mass flow from the incoming canyon ($\dot{m}_{in} = c_{in}Q_{in}$) is lower than the mass flow toward the outgoing canyon ($\dot{m}_{out} = c_{out}Q_{out}$). In order for the mass balance to be satisfied, an external mass flow ($\dot{m}_{ext}$) from the atmosphere above the canopy enters the intersection vertically with an air flow rate $Q_{ext}$ and a concentration $c_{ext}$. Since it is assumed that the external concentration $c_{ext}$ is negligible, this mass flow makes a zero contribution in the mass balance and $c_{out}$ is given by $c_{out} = c_{in}Q_{in}/Q_{out}$. As the flow rate balance in the intersection is $Q_{in}+Q_{ext} = Q_{out}$, the ratio $Q_{in}/Q_{out}$ is lower than 1 and thus $c_{out} < c_{in}$. In the second case, $\dot{m}_{in} > \dot{m}_{out}$ and the flow $\dot{m}_{ext}$ leaves the intersection vertically. We consider that the concentration leaving the intersection is the same for both the upwards flow and the flow towards the outgoing street canyon, i .e. $c_{ext} = c_{out}$. Applying the mass ($c_{in}Q_{in} = c_{out}Q_{out} + c_{ext}Q_{ext}$) and flow rate ($Q_{in} = Q_{out}+Q_{ext}$) balance equations, we find that $c_{out} = c_{in}$. These arguments therefore show that our approach is condervative, i.e. tends to maximise the pollutant concetration in the downwind streets.

Similarly, in case of several streets crossing, we will affect the same concentration at the upwind section of all streets placed downwind the intersection. In other words, we are assuming that the pollutant puff reaching the intersection from a generic street will have a same probability of entering in any of the streets placed downwind the intersection. In doing so, we will consider the trajectories of all possible paths of the pollutant puffs that travel downwind their emission

point.

The assumptions adopted for the transport in street intersections are clearly illustrated in Fig.1c. The contaminated flow from street $(s, i)$ propagates towards streets $(i, j)$ and $(i, k)$. The street $(g, i)$ is unspoiled, as it is shielded from the wind that blows through the source of pollution. According to this scheme, the concentration at the beginning of streets $(i, j)$ and $(i, k)$ is the one at the end of street $(s, i)$.

## 3. A network perspective

In the model presented above, toxic substances move in the urban environment driven by the wind blowing along the street canyons. The street canyons behave like upward leaking transport channels and their geometry, position and connectivity strongly influence the propagation. In big cities, streets cross each other to compose intricate patterns (Fig. 2). Given the spatial extent and the high number of elements, these urban fabrics can be seen as complex networks (Porta et al., 2006; Barthélemy, 2011). Links stand for the street canyons, while nodes represent the street intersections. The direction and the weight of the links describe the geometric and fluid-dynamics properties of the street canyons. Within this approach, the tools of network theory provide interesting information about the propagation phenomena.

### *3.1. Construction of the network*

The urban canopy is modelled as a network of $N$ nodes (intersections) and $M$ links (streets). Fictitious nodes can be created to divide a street into two links in case there is a significant change in the street properties. Each link is directed according to the orientation of the mean wind along the street ($u_{st}$). Thus, the network structure represents both the topological properties of the urban fabric and the directions in which the propagation processes take place. The connectivity of the street canyons is described by the adjacency matrix $\mathbf{A}$, a $N \times N$ square matrix whose element $A_{ij}$ is equal to 1 if a directed link from

node $i$ to node $j$ exists, is equal to 0 otherwise (see Appendix C for an example of adjacency matrix). Since the links have a specific direction, the adjacency matrix is asymmetric.

According to this network representation, the geometry and fluid-dynamics properties of the street canyons are stored efficiently in matrices. $\mathbf{L}$ and $\mathbf{H}$ are the symmetrical matrices of the length of the streets ($l$) and the average height of the buildings overlooking the streets ($h$). The wind velocity along the streets ($u_{st}$) and the velocity of the vertical transfer towards the external atmosphere ($u_d$) are enclosed in the matrices $\mathbf{U}$ and $\mathbf{U_d}$.

As mentioned in the Introduction, the main purpose of this work is to establish a methodology for the rapid assessment of urban vulnerability to the ground-level release of toxic gases. The vulnerability index ($V_s$) for a generic node $s$ can be defined as the number of people affected by the toxic propagation if the release takes place in $s$. The adopted network approach and matrix notation make it easy to calculate $V_s$ as follows,

$$V_s = \sum_{i}^{N} \sum_{j}^{N} D_{ij} P_{ij}, \tag{4}$$

where $\mathbf{P}$ is the matrix that associates at each link $(i, j)$ the number of inhabitants per unit street length and $\mathbf{D}$ is the matrix that associates at each link $(i, j)$ the contaminated length of the street. This last matrix represents the zone of influence of the source node. The meaning of this matrix and its construction process will be widely described in Subsections 3.2 and 3.3.

An interesting advantage of this compact notation is that changes to the network properties can be easily implemented. By modifying matrices $\mathbf{U}$ and $\mathbf{U_d}$, we can simulate different meteorological scenarios, while variations in population distribution (e.g., differences between weekdays and holidays) can be considered by adjusting $\mathbf{P}$. Furthermore, new buildings and structural changes are included in the model by revising the single elements of $\mathbf{L}$ and $\mathbf{H}$.

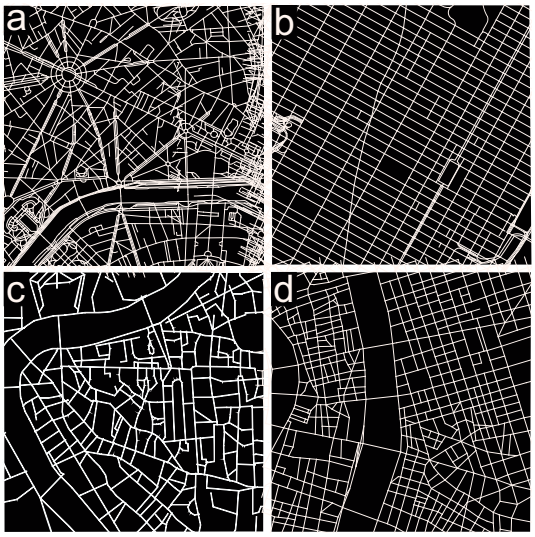


Figure 2: Snapshot of the street network of Paris (a), New York (b), Rome (c), and Lyon (d).

### *3.2. Propagation of a toxic substance in the street network*

Consider the release of a toxic substance in a street intersection (see Fig. 3.a). According to the hypothesis of our model (Section 2), (i) the substance propagates along the adjacent streets depending on the direction of the wind, (ii) the concentration decays exponentially along the streets, (iii) the concentration at the end of each street can be estimated using (3), (iv) the concentration remains unchanged in the street intersections, and (v) from a contaminated street intersection the gas spreads further to the adjacent streets.

Given this description, the pollutant dispersion within the canopy can be then easily seen as a spreading process on a network (e.g., Newman, 2002; Comin and da Fontoura Costa, 2011). In Fig. 3.b the urban canopy is represented as a network. The links are directed according to the direction of the wind in the streets and the release is modelled as a source node $s$. From a network perspective, transport from $s$ towards a generic node $u$ is possible if there is a link directed from $s$ to $u$, i.e. if (i) the two nodes are physically connected by a street canyon, and (ii) the wind is blowing from the source towards the target node. Once infected, the target node $u$ is modelled as a new source

and the spreading process carries on towards the farthest nodes. According to this scheme, propagation is a recursive process that spontaneously expands to the topological boundaries of the network. Physically, the extent of the contaminated zone can be delimited based on a threshold concentration value $c_{th}$: when the concentration falls below $c_{th}$, the contamination process is irrelevant. Thus, a stopping rule for the spreading process on the network is introduced: at each propagation hop the concentration at the target node is estimated. If this concentration is higher than $c_{th}$, then the propagation carries on.

Considering the example in Fig. 3.b, a toxic substance is released in the source node $s = 15$ and propagates towards the first neighbours of $s$: nodes 10, 11, and 16. The concentration in the first neighbours is evaluated using Equation (3), as a function of the geometric and wind characteristics of the street canyons associated to links $(15, 10)$, $(15, 11)$ and $(15, 16)$. Since the concentration in the first neighbours is grater than the predefined threshold $c_{th}$, nodes 10, 11 and 16 act as source nodes and the spreading process carries on towards the second neighbours of $s$. In the same way, the third and fourth neighbours are affected by the toxic propagation until the concentration in the nodes falls below $c_{th}$.

According to this network interpretation, the spreading of a toxic gas in the urban environment is governed by two properties of the network: (i) the topological connectivity of the network, given by its adjacency matrix $\mathbf{A}$, and (ii) the concentration decay along the links, given by a combination of the geometric characteristics and the flow dynamics in the street canyons.

This spreading results in the zone of influence of the source node $s$, i.e. the set of links contaminated from the propagation process originated in $s$ (the elements highlighted in blue in Fig. 3). The number of people that lives in the zone of influence represents the vulnerability index of $s$ ($V_s$). Notice that this index contains both information on population density and meteorological conditions in the city. In fact, as will be shown in the following sections, its value changes drastically with the wind direction.

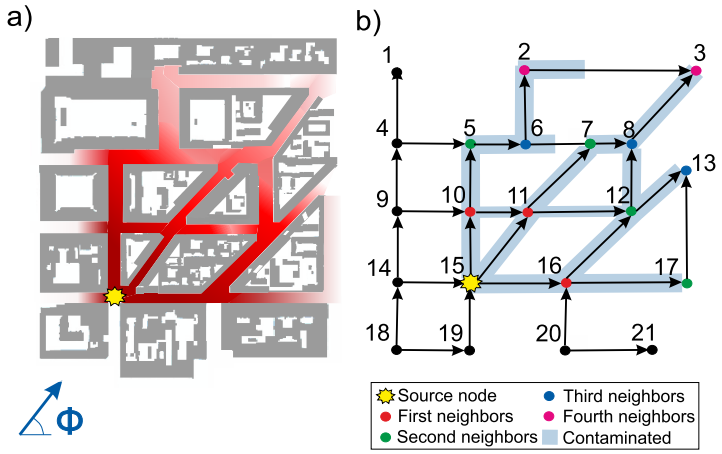


Figure 3: Analogy between the physical propagation of a toxic substance in the urban environment (a) and the spreading process on a network (b). $\Phi$ is the direction of the external wind blowing on the city.

### *3.3. Algorithm*

Given a source node $s$ with a concentration $c_s$, the set of its first neighbours $N_1(s)$ can be derived from the non-zero elements of the $s-th$ row of the adjacency matrix $\mathbf{A}$. In Fig. 3, $s = 15$ and thus $N_1(s) = \{10, 11, 16\}$. For each node $u$ belonging to the set $N_1(s)$, the algorithm calculates the distance $D_{su}^{pot}$. This length is the potential distance (hence the superscript *pot*) that the contaminated front can reach along the link $(s, u)$ with a concentration higher than the predefined threshold $c_{th}$. According to (3), $D_{su}^{pot}$ is

$$D_{su}^{pot} = -\frac{H_{su}}{U_{d,su}} U_{su} \log\left(\frac{c_{th}}{c_s}\right), \quad \forall u \in N_1(s). \tag{5}$$

In general, $D_{su}^{pot}$ is different from the physical length of the street ($L_{su}$) associated to the link $(s, u)$. $D_{su}^{pot}$ is lower than $L_{su}$ if the concentration undergoes the threshold $c_{th}$ before the propagation front has travelled the entire street. *Vice versa*, it is higher if the front reaches node $u$ with a concentration above the threshold. As a consequence, the effective contaminated distance ($D_{su}$) is the minimum between the reachable distance $D_{su}^{pot}$ and the effective length of

the street, i.e.

$$D_{su} = \min[D_{su}^{pot}, L_{su}] \tag{6}$$

If $D_{su} = L_{su}$, the substance has reached the target node $u$ with a concentration equal to or higher than $c_{th}$. As a result, node $u$ is contaminated. Conversely, if the front reaches $u$ with a negligible concentration (i.e. $D_{su} < L_{su}$), then node $u$ remains unspoiled. In both cases, the algorithm stores the effective contaminated length $D_{su}$ as the $(s, u)$ element in the matrix $\mathbf{D}$. As introduced in Section 3.1, this matrix defines the zone of influence of the source node $s$.

We define $\hat{N}_1(s)$ the set of the first neighbours of $s$ that have been contaminated,

$$\hat{N}_1(s) = \{u \in N_1(s) \mid D_{su} = L_{su}\}. \tag{7}$$

Referring to Fig. 3, $\hat{N}_1(15) = \{10, 11, 16\}$ since all the first neighbours of $s$ are contaminated. The algorithm estimates the concentration in the nodes belonging to $\hat{N}_1(s)$ using (3), as

$$c_u = c_s e^{-\frac{U_{d,su}}{H_{su}} \frac{L_{su}}{U_{su}}}, \qquad \forall u \in \hat{N}_1(s). \tag{8}$$

These nodes behave as new source nodes. Thus, the algorithm repeats the above presented steps, replacing in Equations (5)-(8) node $s$ with the nodes belonging to $\hat{N}_1(s)$. For example, once node 16 (Fig. 3) has been contaminated from the initial source node 15, the algorithm finds the set of its first neighbours, i.e. $N_1(16) = \{12, 17\}$. Equations (5)-(6) estimate the effective contaminated length along links (16, 12) and (16, 17), while (7) identifies the set of the first neighbours of node 16 that have been infected, i.e. $\hat{N}_1(16) = \{12, 17\}$. Finally, the concentration reached in nodes 12 and 17 is determined by (8). This procedure is repeated recursively until the concentration in each node of the network falls below the threshold $c_{th}$.

Notice that for nodes 15 and 16 the sets $N_1$ and $\hat{N}_1$ are identical. However,

this is not true in general. Consider node 6 in Fig. 3b. The set of its first neighbours is $N_1(6) = \{2, 7\}$, while $\hat{N}_1(6) = \{2\}$ because node 7 cannot be reached by the propagation along link (6, 7).

The algorithm explores the nodes of the network starting from a root node and progressively visiting the adjacent nodes. In computer science, this process is called tree traversal (Valiente, 2013) since the result of the exploration is a tree structure that is a subgraph of the initial graph. In our study, this tree corresponds to the zone of influence of the source node. There are multiple ways to perform a tree traversal, according to the order in which the nodes are visited. The algorithm presented above explores the nodes of the network using a depth-first search analysis. The algorithm starts at the source node and goes as far as it can down a given branch before backtracking. Referring to Fig. 3, the algorithm starts at node 15, selects the first node 10 in the set $\hat{N}_1(15)$ and deepens the analysis in the first element of the set $\hat{N}_1(10)$, i.e. node 5. Following this ratio, the algorithm visits the nodes in the order (15, 10, 5, 6, 2). The in-depth analysis along this path ends when the concentration falls below the threshold $c_{th}$. Formally, the path (15, 10, 5, 6, 2) ends because the set $\hat{N}_1(2)$ is empty. Once the first branch has been explored, the algorithm backtracks to node 6's next available neighbour, i.e. node 7.

From the numerical point of view, depth-first search analysis requires less memory and it is more efficient in finding trees on networks compared to other algorithms, such as breath-first search (Kozen, 1992).

Notice that, referring to the example in Fig. 3b, link $(11, 7)$ is affected by toxic propagation twice, both along propagation path $\gamma_1$=(15, 11, 7) and $\gamma_2$=(15, 10, 11, 7). As a consequence the algorithm calculates two different values of $D_{11,7}$, since the concentration reached at node 11 ($c_{11}$) along $\gamma_1$ is generally different from the one obtained along $\gamma_2$. As the aim of the elaboration is to determine the extent of the zone of influence, the algorithm considers all the possible passages through a generic link and stores the longest distance reached by the toxic substance. In details, for each path $\gamma_\alpha$ the algorithm compares

$D_{su}^{(\gamma_\alpha)}$ with the distance $D_{su}^{(\gamma_{\alpha-1})}$ obtained along the previously explored path $\gamma_{\alpha-1}$ passing through the link $(s, u)$. Equation (6) is, thus, refined as:

$$D_{su}^{(\gamma_\alpha)} = \max[\min[D_{su}^{pot}, L_{su}], D_{su}^{(\gamma_{\alpha-1})}], \tag{9}$$

where $\gamma_\alpha$ is an index for the order in which the path is explored.

## 4. Results

The potentials of the proposed approach are discussed through a case study. The model is applied to assess urban vulnerability of the city of Lyon (France) to the release of a toxic gas. Lyon (Fig. 4) is located in east-central France and it is the third-largest urban agglomeration in France after Paris and Marseille, with a population of approximately 1.5 million inhabitants. In this work, the analysis is limited to a part of the city (Fig. 4c) that presents an intricate urban fabric and tall buildings on the edge of the streets. These characteristics are consistent with the model representation of the streets as a network of street canyons. The study area has an extent of about 6.5 $km^2$, it hosts a population of about 140,000 inhabitants and is delimited by natural and artificial boundaries (rivers, parks and railways). These boundaries determine a discontinuity in the dispersion of pollutants along the street canyons.

The street canyons and the street intersections result in a network of 750 nodes and 1110 links. The geometric characteristics of the street canyons, the population density, the longitudinal mean wind and the vertical transfer velocity in the streets are stored in the matrices $\mathbf{H}$, $\mathbf{L}$, $\mathbf{P}$, $\mathbf{U}$ and $\mathbf{U_d}$, respectively.

### *4.1. The zone of influence of a source node*

The first outcome of the elaboration is the identification of the zone of influence of a source node, i.e. the set of links contaminated by the toxic substance with a concentration above a defined threshold, stored in matrix $\mathbf{D}$ (see Section 3).

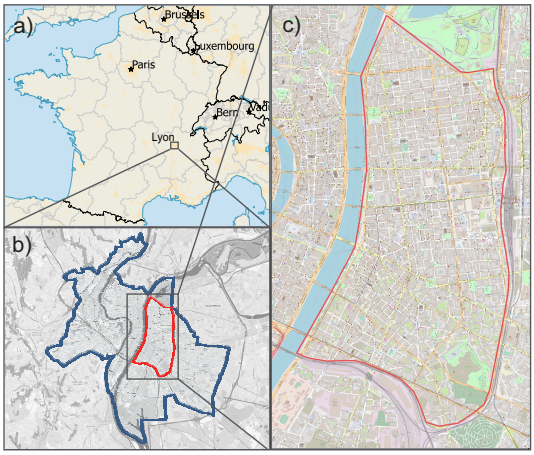


Figure 4: The case study area. a) Location of the metropolitan area of Lyon within France. b) Location of the study area within the municipality of Lyon. c) The study area.

As an example, Fig. 5 shows the zone of influence of a source node for different wind directions ($\Phi = 45°$, 135°, 225° and 315°) and for two different initial concentration values. For the sake of generality, the concentration scenarios are defined by the ratio between the concentration in the source node ($c_0$) and the limit concentration ($c_{th}$).

The urban topology, the wind direction and the initial concentration shape the zone of influence of the source node. Variations in the mean velocity of the external wind ($\overline{u}$) as well as the stability conditions (as determined by the Monin-Obukhov length $L_{MO}$) are instead irrelevant. As stated in (2) and (A.1)-(A.2), both $u_d$ and $u_{st}$ linearly depend on the friction velocity $u_*$. Since our propagation model evaluates the pollutant spreading as a function of their ratio (3), variations of $u_*$, and thus of $L_{MO}$ and $\overline{u}$, will not be effective in determining the zone of influence.

### *4.2. Spatial and frequency distribution of urban vulnerability*

The spatial pattern of urban vulnerability can be analysed at a glance using vulnerability maps. Given the geometry of the urban fabric, the conditions of the external wind, the spatial distribution of the citizens and the emission scenario, the model provides in a short time (from a few seconds to a few minutes

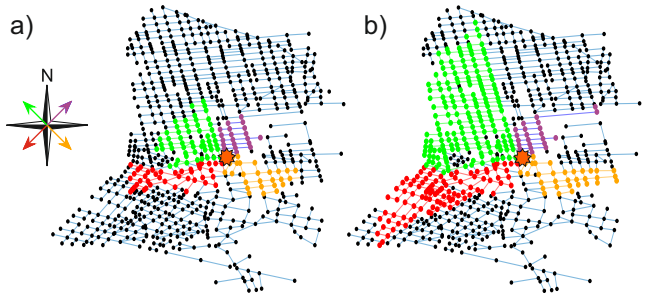


Figure 5: The zone of influence of a generic source node (orange star) in the network for different wind directions (red, green, violet and yellow refer to the wind directions $\Phi = 45°$, $135°$, $225°$ and $315°$, respectively). Panel (a) and (b) refer to a concentration ratio $c_0/c_{th} = 10$ and $c_0/c_{th} = 100$, respectively.

depending on the concentration ratio $c_0/c_{th}$) a map that associates at each node of the street network its vulnerability index. To do this, the algorithm for the spread of toxic substances on networks (Section 3) is applied and the matrix of the contaminated street lengths $\mathbf{D}$ (i.e. the zone of influence) is computed for all nodes of the network. Next, the vulnerability index defined in Equation (4) is calculated for each node, taking into account both the extent of the zone affected by the propagation originated in the node ($\mathbf{D}$) and the number of people leaving in that zone ($\mathbf{P}$). Finally, a vulnerability map is constructed by associating a colour to each node based on its vulnerability index.

Sixteen vulnerability maps for the case study area are obtained (see the supplementary material) by varying the direction of the external wind ($\Phi$) and the concentration ratio $c_0/c_{th}$. These parameters affect the node vulnerability by shaping its zone of influence (matrix $\mathbf{D}$), as mentioned in Section 4.1. In this study, the number of inhabitants in the streets ($\mathbf{P}$) was kept constant in the different scenarios and was derived from the map of the resident citizens in the city of Lyon. Future works should consider how the spatial distribution of the population varies on different days of the week or at different times of the day. These variations could be easily implemented in the model by modifying the $\mathbf{P}$ matrix and would increase the number of cases (i.e. maps) considered.

Fig. 6 shows four vulnerability maps for a wind direction varying between $\Phi = 0°$ (north wind) and $\Phi = 135°$. The maps are obtained simulating for

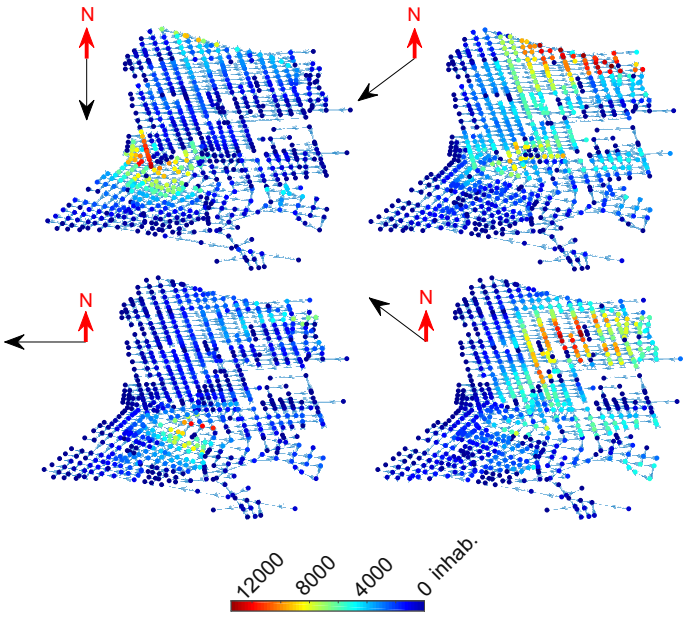


Figure 6: Vulnerability maps for different wind directions and with a concentration ratio $c_0/c_{th}$ equal to 10.

each node a release with a concentration equal to ten times the threshold value, i.e. $c_0/c_{th} = 10$. Node vulnerability, defined in terms of affected people, varies between 0 (blue) and 12000 (red) inhabitants. The maps reveal at a glance the most susceptible areas and the global vulnerability of the urban fabric in the different wind direction scenarios. From Fig. 6, it can be seen that the vulnerability index is not distributed homogeneously. On the contrary, the vulnerability tends to be maximal (red nodes) in a defined area of the map and its value gradually decreases in the nodes around it. Moreover, the position of the most vulnerable nodes varies strongly with small variations in the wind direction. As an example, notice the difference between the two scenarios related to $\Phi = 0°$ and $\Phi = 45°$ in Fig. 6.

To better understand this behaviour, Fig. 7.a summaries the results of the sixteen simulated scenarios. Each scenario is represented by an arrow oriented with the wind direction, coloured according to the concentration ratio and positioned in the area of greatest vulnerability for that scenario. It is evident that

for $\Phi$ equal to 0°, 90°, 180° and 270° (the cardinal directions) the most vulnerable nodes are located in the southern part of the network, while for $\Phi$ equal to 45°, 135°, 225° and 315° (the transversal directions) the most vulnerable areas are in the northern part of the network.

As the geometric characteristics of the street canyons and the population density are rather homogeneously distributed in the street network, this different vulnerability pattern is related to the orientation of the streets with respect to the wind direction. The northern part of the street network is mainly oriented according to the cardinal directions (North-South and West-East oriented streets). As the wind blows in one of these directions (e.g., $\Phi = 0°$), only the aligned streets (i.e. the North-South oriented streets) are affected by the propagation of toxic substances, while the orthogonal streets (i.e. the East-West oriented streets) are completely shielded from the wind. This condition limits the extent of the zone of influence of a generic source node. Conversely, as the wind blows according to one of the transversal direction, the propagation affects both the North-South and the East-West oriented streets, thus increasing the vulnerability. As the southern part of the street network is oriented mainly according to the transverse directions, a greater vulnerability will occur when the wind is blowing in the cardinal directions.

For each of the sixteen scenarios analysed, the average vulnerability over the entire network ($\overline{V}$) is calculated as

$$\overline{V} = \frac{1}{N} \sum_{i}^{N} V_i, \tag{10}$$

where $V_i$ is the vulnerability index for the $i-th$ node and $N$ is the number of nodes in the network. The two polar histograms of Fig. 7.b report these average vulnerability values for the two concentration ratios considered. Each sector in the polar histograms refers to a different wind direction. As expected, higher concentration ratios correspond to higher vulnerability values. Moreover, since most of the streets ($\sim 60\%$) are oriented in the cardinal directions, the average vulnerability is greater when the wind blows in the transversal directions.

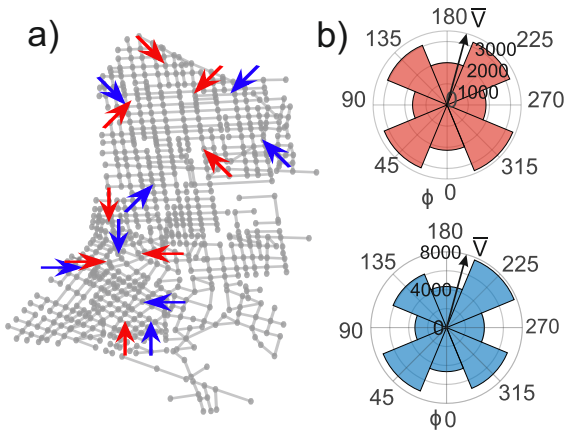


Figure 7: a) Most vulnerable areas in the street network for different wind directions and concentration ratios. Each scenario is represented by an arrow oriented according to the wind direction, coloured according to the concentration ratio (red arrows for $c_0/c_{th} = 10$ and blue arrows for $c_0/c_{th} = 100$) and positioned in the area of greatest vulnerability on the map. b) Polar histogram (red for $c_0/c_{th} = 10$ and blue for $c_0/c_{th} = 100$) of the average node vulnerability for the different wind directions

Fig. 8 gives an overview of the long-term vulnerability of the urban fabric to toxic releases. The maps depict nodes vulnerability weighted by the annual frequency of the wind directions over the city of Lyon. As detailed in the inset of Fig. 8, the dominant wind direction in Lyon is North-South. As a consequence, the highest vulnerabilities are located in the circled area, corresponding to the regions mostly stressed by North-South oriented winds (see $\Phi = 0°$ and $\Phi = 180°$ scenarios in the supplementary material).

Results in Fig. 6 suggest that, for each scenario, a restricted area of the urban fabric is characterized by high levels of vulnerability, while most of the streets are not exposed. Thus, both spatial and frequency distribution of node vulnerabilities are not trivial. A frequency analysis of vulnerability values was performed to identify an eventual significant statistical distribution of the data. For each scenario, node vulnerability values were classified in ten equal size intervals. Then, the relative frequency ($p$) of each class was calculated. Fig. 9

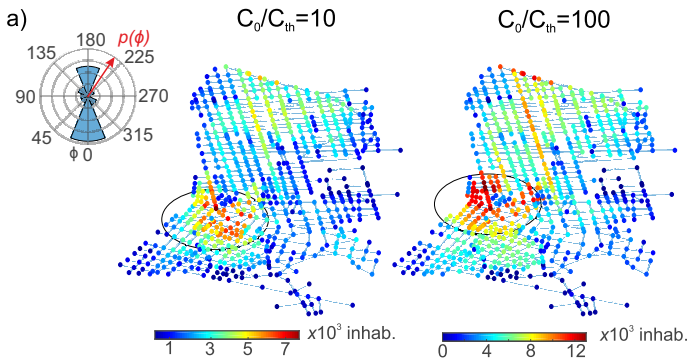


Figure 8: Maps of vulnerability weighted by the annual frequency of the wind directions. The polar histogram (inset *a*) shows the occurrence of wind directions in the city of Lyon in terms of annual relative frequency $p(\Phi)$.

presents the relative frequency of node vulnerability for the different scenarios in a log-log plot. For the sake of graphic clarity, vulnerability values were normalised to the maximum one ($V_{max}$). Generally, the data show a linear behaviour in the log-log plot, thus exhibiting a power law trend. The power law confirms that vulnerability distribution is heterogeneous, with few nodes being much more critical than the others. This hierarchical configuration suggests that, for each wind scenario, the entire neighbourhood could be protected with security interventions targeted on small urban areas.

Notice that many real-world networks (e.g., the Internet, World Wide Web, scientific citations) present a power law distribution of nodes degree (Boccaletti et al., 2006). The degree defines the importance of a node in the network in terms of its connectivity. In this case, a power law results from the not trivial interaction of multiple factors that define the vulnerability index, i.e. the topological connectivity of the network, the geometry characteristics of the street canyons, the toxic spreading process and the population distribution in the city.

## 5. Conclusions

We have presented an innovative approach for the study of diffusion processes in the urban atmosphere. Within the urban canopy, the wind flows along

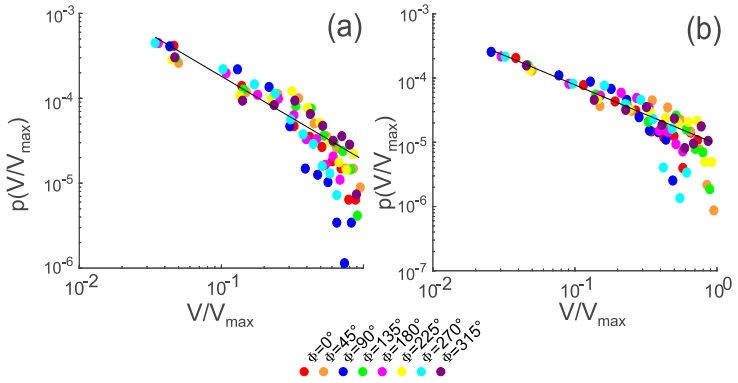


Figure 9: Relative frequency of vulnerability for different wind directions and for a concentration ratio $c_0/c_{th} = 10$ (a) and $c_0/c_{th} = 100$ (b). The display is in logarithmic scale.

the street canyons and the transport of pollutants is strongly influenced by the structure of the city, i.e. by the orientation of the streets and by their interconnections. Moving from these considerations, we have modelled the interaction between the city and the external wind as a weighted complex network whose links and nodes represent the streets and the street intersections, respectively. The direction of the links and their weights describe the direction and the intensity of the wind along the streets and the geometric properties of the buildings that surround the street canyons. Using a depth-first search analysis, we have implemented a spreading model on networks that simulates the propagation process from a point source. As an example, the developed method has been adopted to create vulnerability maps of the city of Lyon (France). These maps highlight the most vulnerable areas of the city, i.e. the areas from which the spread of a toxic substance, released at ground level, can damage more people. We found that the spatial and frequency distribution of urban vulnerability is heterogeneous and is strongly influenced by the alignment between the direction of the external wind and the orientation of the streets.

The model proved to be quick and functional and therefore useful for the analysis of multiple scenarios that take into account various meteorological conditions or different distributions of the residing population. Thanks to these characteristics, this method is suitable for the prediction and management of

emergency scenarios, due to accidental or harmful releases of toxic substances in the urban atmosphere.

This work is in line with recent efforts to develop operational modelling tools for the prediction of pollutant transport in large urban areas. Moreover, the study demonstrate that the innovative tools of the theory of complex networks can be adopted to this aim. The frequency with which new techniques and applications are developed in the field of complex networks makes this new perspective particularly promising.

Future work is aimed at comparing different cities to understand how urban topology influences the diffusive process and therefore the vulnerability of the city. In this way, it will be possible to understand which cities are the most structurally fragile. Further analyses should be conducted to consider variations in urban vulnerability due to changes in the presence of people in the different times of the day or during the different periods of the week. Finally, the results encourage a deeper understanding of the link between the theory of complex networks and the problems of diffusion in the urban environment.

## Appendix A. Longitudinal wind velocity along a street canyon

According to Soulhac et al. (2008), the average velocity $u_{st}$ along the longitudinal axis of a street canyon reads

$$u_{st} = u_H \cos\Phi \frac{\delta_i^2}{hw} \left[ \frac{2\sqrt{2}}{C}(1-\beta)\left(1 - \frac{C^2}{3} + \frac{C^4}{45}\right) + \beta\frac{2\alpha - 3}{\alpha} + \left(\frac{w}{\delta_i} - 2\right)\frac{\alpha - 1}{\alpha} \right] \tag{A.1}$$

$$\text{with} = \begin{cases} \alpha = \ln\left(\frac{\delta_i}{z_{0,build}}\right) \\ \beta = \exp\left[\frac{C}{\sqrt{2}}\left(1 - \frac{h}{\delta_i}\right)\right] \\ u_H = u_* \sqrt{\frac{\pi}{\sqrt{2}k^2 C}\left[Y_0(C) - \frac{J_0(C)Y_1(C)}{J_1(C)}\right]} \\ C \text{ solution of } \frac{z_{0,build}}{\delta_i} = \frac{2}{C}\exp\left[\frac{\pi}{2}\frac{Y_1(C)}{J_1(C)} - \gamma\right] \\ \delta_i = \min\left(h, \frac{w}{2}\right) \end{cases} \tag{A.2}$$

where $\Phi$ is the external wind direction with respect to the street longitudinal axis, $h$ and $w$ are the height and the width of the street canyon, $z_{0,build}$ is the aerodynamic roughness of the canyon walls, $u_*$ is the friction velocity of the external atmospheric boundary layer flow, $J_0$, $J_1$, $Y_0$ and $Y_1$ are Bessel functions, $k$ is the von Kármán constant, and $\gamma$ is the Euler constant. The friction velocity $u_*$ is determined using the Monin-Obukhov similarity theory to model the flow in the external boundary layer.

## Appendix B. Solution for the one-dimensional transport equation

Under the assumption that $c_{ext}$ is negligible with respect to the concentration in the street canyon, the one-dimensional transport equation (1) becomes

$$\frac{\partial c}{\partial t} + u_{st}\frac{\partial c}{\partial x} + \frac{u_d}{h}c = 0. \tag{B.1}$$

By introducing the substitution

$$g(x,t) = c(x,t)\exp\left(\frac{u_d}{h}t\right), \tag{B.2}$$

(B.1) yields

$$\frac{\partial g}{\partial t} + u_{st}\frac{\partial g}{\partial x} = 0. \tag{B.3}$$

The general solution for (B.3) is found by introducing the new coordinates $\tau = t$, $\xi = x - u_{st}t$ and using the chain rule:

$$\frac{\partial g(x,t)}{\partial t} = \frac{\partial g(\xi,\tau)}{\partial \tau} - u_{st}\frac{\partial g(\xi,\tau)}{\partial \xi} \tag{B.4}$$

$$\frac{\partial g(x,t)}{\partial x} = \frac{\partial g(\xi,\tau)}{\partial \xi}. \tag{B.5}$$

607 Equation (B.3) becomes

$$\frac{\partial g(\xi,\tau)}{\partial \tau} = 0, \tag{B.6}$$

608 and, therefore,

$$g(\xi,\tau) = F(\xi) \qquad \rightarrow \qquad g(x,t) = F(x - u_{st}t), \tag{B.7}$$

609 where $F$ is a derivable function. The solution of (B.1) is obtained returning to
610 the original function,

$$c(x,t) = g(x,t)\exp\left(-\frac{u_d}{h}t\right) = F(x - u_{st}t)\exp\left(-\frac{u_d}{h}t\right). \tag{B.8}$$

611 Function $F$ is found using the initial or boundary conditions of the problem.
612 For a continuous release $c_0$ in the source node starting from $t \geq 0$, the
613 boundary condition is defined as

$$c(0,t) = c_0\Theta(t), \tag{B.9}$$

614 where $\Theta$ is the Heaviside function. For $x = 0$, (B.8) and (B.9) yield

$$c(0,t) = F(-u_{st}t)\exp\left(-\frac{u_d}{h}t\right) = c_0\Theta(t). \tag{B.10}$$

615 Function $F$ is obtained from the previous one and the solution for the continuous
616 release is thus

$$c(x,t) = F(x - u_{st}t)\exp\left(-\frac{u_d}{h}t\right) = c_0\exp\left(-\frac{u_d}{u_{st}}\frac{x}{h}\right)\Theta\left(t - \frac{x}{u_{st}}\right). \tag{B.11}$$

For a quick release in the source node, the initial condition is set as a rectangular pulse with width $a$ and height $c_0$

$$c(x,0) = c_0[\Theta(x) - \Theta(x-a)]. \tag{B.12}$$

When $a$ tends to zero, the release is almost instantaneous. Following the same reasoning as in (B.10) and (B.11), but considering this time $t = 0$, we obtain the solution for a quick release:

$$c(x,t) = c_0 \exp\left(-\frac{u_d}{h}t\right)[\Theta(x - u_{st}t) - \Theta(x - u_{st}t - a)]. \tag{B.13}$$

## Appendix C. Adjacency matrix

Consider the network in Fig.1c, extracted as a subgraph from the network of streets in Fig.1a. The adjacency matrix of this simple four-links graph reads

$$\mathbf{A} = \begin{array}{c} \\ s \\ g \\ i \\ j \\ k \end{array} \begin{array}{c} \begin{array}{ccccc} s & g & i & j & k \end{array} \\ \begin{pmatrix} 0 & 0 & 1 & 0 & 0 \\ 0 & 0 & 1 & 0 & 0 \\ 0 & 0 & 0 & 1 & 1 \\ 0 & 0 & 0 & 0 & 0 \\ 0 & 0 & 0 & 0 & 0 \end{pmatrix} \end{array}. \tag{C.1}$$

Note that the matrix is asymmetric since the network is directed (i.e. the links have a specific direction).

## References


Ahern, J., 2011. From fail-safe to safe-to-fail: Sustainability and resilience in the new urban world. Landscape and Urban Planning 100 (4), 341–343.

Arnfield, A. J., 2003. Two decades of urban climate research: A review of turbulence, exchanges of energy and water, and the urban heat island. International Journal of Climatology 23 (1), 1–26.

633 Barthélemy, M., 2011. Spatial networks. Physics Reports 499 (1-3), 1–101.

634 Berke, P. R., Song, Y., Stevens, M., 2009. Integrating hazard mitigation into
635 new urban and conventional developments. Journal of Planning Education
636 and Research 28 (4), 441–455.

637 Blocken, B., 2015. Computational Fluid Dynamics for urban physics: Impor-
638 tance, scales, possibilities, limitations and ten tips and tricks towards accurate
639 and reliable simulations. Building and Environment 91, 219–245.

640 Boccaletti, S., Latora, V., Moreno, Y., Chavez, M., Hwang, D.-U., 2006. Com-
641 plex networks: Structure and dynamics. Physics Reports 424 (4-5), 175–308.

642 Borgatti, S. P., Mehra, A., Brass, D. J., Labianca, G., 2009. Network analysis
643 in the social sciences. Science 323 (5916), 892–895.

644 Brunekreef, B., Holgate, S. T., 2002. Air pollution and health. The Lancet
645 360 (9341), 1233–1242.

646 Carruthers, D., Edmunds, H., Lester, A., McHugh, C., Singles, R., 2000. Use
647 and validation of ADMS-Urban in contrasting urban and industrial locations.
648 International Journal of Environment and Pollution 14 (1-6), 364–374.

649 Carvalho, R., Buzna, L., Bono, F., Gutiérrez, E., Just, W., Arrowsmith, D.,
650 2009. Robustness of trans-European gas networks. Physical Review E 80 (1),
651 016106.

652 Comin, C. H., da Fontoura Costa, L., 2011. Identifying the starting point of a
653 spreading process in complex networks. Physical Review E 84 (5), 056105.

654 Di Sabatino, S., Buccolieri, R., Salizzoni, P., 2013. Recent advancements in
655 numerical modelling of flow and dispersion in urban areas: A short review.
656 International Journal of Environment and Pollution 7 52 (3-4), 172–191.

657 Gelbrecht, M., Boers, N., Kurths, J., 2017. A complex network representation of
658 wind flows. Chaos: An Interdisciplinary Journal of Nonlinear Science 27 (3),
659 035808.

660 Giustolisi, O., Ridolfi, L., 2014. A novel infrastructure modularity index for
661 the segmentation of water distribution networks. Water Resources Research
662 50 (10), 7648–7661.

663 Heinrich, J., Wichmann, H.-E., 2004. Traffic related pollutants in Europe and
664 their effect on allergic disease. Current Opinion in Allergy and Clinical Im-
665 munology 4 (5), 341–348.

666 Hunter, L. J., Watson, I., Johnson, G., 1990. Modelling air flow regimes in urban
667 canyons. Energy and Buildings 15 (3-4), 315–324.

668 Kozen, D. C., 1992. Depth-first and breadth-first search. In: The Design and
669 Analysis of Algorithms. Springer, pp. 19–24.

670 Mayer, H., 1999. Air pollution in cities. Atmospheric Environment 33 (24-25),
671 4029–4037.

672 McLeish, C., 2017. Recasting the threat of chemical terrorism in the EU: The is-
673 sue of returnees from the syrian conflict. European Journal of Risk Regulation
674 8 (4), 643–657.

675 Namdeo, A., Colls, J., 1996. Development and evaluation of SBLINE, a suite of
676 models for the prediction of pollution concentrations from vehicles in urban
677 areas. Science of the Total Environment 189, 311–320.

678 Newman, M., 2010. Networks: An introduction. Oxford university press.

679 Newman, M. E., 2002. Spread of epidemic disease on networks. Physical Review
680 E 66 (1), 016128.

681 Oke, T. R., 1982. The energetic basis of the urban heat island. Quarterly Journal
682 of the Royal Meteorological Society 108 (455), 1–24.

683 Porta, S., Crucitti, P., Latora, V., 2006. The network analysis of urban streets:
684 A dual approach. Physica A: Statistical Mechanics and its Applications
685 369 (2), 853–866.

686 Robins, A., Savory, E., Scaperdas, A., Grigoriadis, D., 2002. Spatial variability
687 and source-receptor relations at a street intersection. Water, Air and Soil
688 Pollution: Focus 2 (5-6), 381–393.

689 Roth, M., 2000. Review of atmospheric turbulence over cities. Quarterly Journal
690 of the Royal Meteorological Society 126 (564), 941–990.

691 Salizzoni, P., Soulhac, L., Mejean, P., 2009. Street canyon ventilation and at-
692 mospheric turbulence. Atmospheric Environment 43 (32), 5056–5067.

693 Ser-Giacomi, E., Rossi, V., López, C., Hernandez-Garcia, E., 2015. Flow net-
694 works: A characterization of geophysical fluid transport. Chaos: An Interdis-
695 ciplinary Journal of Nonlinear Science 25 (3), 036404.

696 Soulhac, L., Garbero, V., Salizzoni, P., Mejean, P., Perkins, R., 2009. Flow and
697 dispersion in street intersections. Atmospheric Environment 43 (18), 2981–
698 2996.

699 Soulhac, L., Perkins, R. J., Salizzoni, P., 2008. Flow in a street canyon for any
700 external wind direction. Boundary-Layer Meteorology 126 (3), 365–388.

701 Soulhac, L., Salizzoni, P., Cierco, F.-X., Perkins, R., 2011. The model SIRANE
702 for atmospheric urban pollutant dispersion; part I, presentation of the model.
703 Atmospheric Environment 45 (39), 7379–7395.

704 Soulhac, L., Salizzoni, P., Mejean, P., Perkins, R., 2013. Parametric laws to
705 model urban pollutant dispersion with a street network approach. Atmo-
706 spheric Environment 67, 229–241.

707 Tominaga, Y., Stathopoulos, T., 2012. CFD modeling of pollution dispersion in
708 building array: Evaluation of turbulent scalar flux modeling in RANS model
709 using LES results. Journal of Wind Engineering and Industrial Aerodynamics
710 104, 484–491.

711 Tucker, J. B., 2000. Toxic terror: Assessing terrorist use of chemical and bio-
712 logical weapons. MIT Press.

Valiente, G., 2013. Algorithms on trees and graphs. Springer Science & Business Media.

Yazdani, A., Jeffrey, P., 2011. Complex network analysis of water distribution systems. Chaos: An Interdisciplinary Journal of Nonlinear Science 21 (1), 016111.

**Supplementary Material**

**Click here to download Supplementary Material: Supplementary_material.pdf**